Quantitative valence bond computation of a curve crossing diagram for a model SN2 reaction, H− + CH3H′ → HCH3 + H′−

ARTICLE *in* THE JOURNAL OF PHYSICAL CHEMISTRY · JULY 1989

Impact Factor: 2.78 · DOI: 10.1021/j100352a007

5 AUTHORS, INCLUDING:

Gjergji Sini
Université de Cergy-Pontoise
31 PUBLICATIONS **570** CITATIONS
SEE PROFILE

Sason Shaik
Hebrew University of Jerusalem
530 PUBLICATIONS **20,909** CITATIONS
SEE PROFILE

Gilles Ohanessian
French National Centre for Scientific Research
115 PUBLICATIONS **3,738** CITATIONS
SEE PROFILE

Philippe C Hiberty
Université Paris-Sud 11
110 PUBLICATIONS **4,028** CITATIONS
SEE PROFILE

quantitative diabatic curves of VB type, for thermal as well as photochemical reactions.

Using basis sets larger than DZ + P does not set any conceptual problem; it would simply increase the number of complementary VBFs and therefore the dimension of the CI. Yet the basis sets used in this work provide reasonably good energetics and have therefore been kept in the following paper in which VB curve-crossing diagrams are calculated.

Quantitative Valence Bond Computations of Curve-Crossing Diagrams for Model Atom Exchange Reactions

P. Maitre, P. C. Hiberty, G. Ohanessian,*

Laboratoire de Chimie Théorique (UA 506 du CNRS), Université de Paris-Sud, 91405 Orsay Cedex, France

and S. S. Shaik*

Department of Chemistry, Ben Gurion University of the Negev, Beer Sheva 84105, Israel
(Received: April 20, 1989; In Final Form: September 26, 1989)

Curve-crossing diagrams are presented and computed for the exchange reactions $X^{\bullet} + X\text{-}X \rightarrow X\text{-}X + X^{\bullet}$, X = H, Li, by use of a multistructure VB approach. The computations provide the essential diagram quantities *G*, *f*, and *B*. These parameters are 156.8 kcal/mol, 0.37, and 42.4 kcal/mol, respectively, for X = H, and 22.4 kcal/mol, 0.13, and 6.6 kcal/mol for X = Li. The quantitative analyses confirm the qualitative deduction that all these quantities are related to a fundamental property of X, the singlet-triplet splitting ΔE_{st}(X-X) of the dimer. It is possible therefore to predict the height of the barrier and the mechanistic modality of the exchange reaction by reliance on ΔE_{st}; as ΔE_{st} decreases in a series the barrier decreases and eventually the X_3 species is converted to a stable intermediate. The *B* quantity is the quantum mechanical resonance energy (QMRE) of the X_3 species. The values of 42.4 kcal/mol for H_3 and 6.6 kcal/mol for Li_3 are computed as energy differences between a variational bonding scheme and the variational adiabatic and delocalized (X-X-X) state.

I. Introduction

Curve-crossing VB diagrams[1,2] are general models for discussing reactivity patterns. In the two-curve model **1** (state correlation diagram, SCD)[2a,b] the reaction profile arises as a consequence of the avoided crossing of two diabatic (or nearly so) curves, one

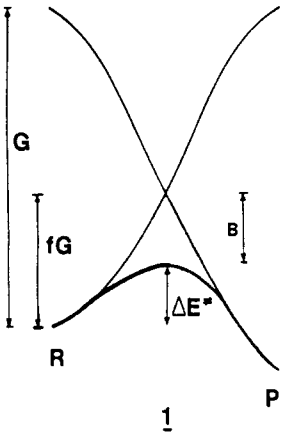

1

representing the bonding scheme of the reactants, the other that of the products. The barrier of the reaction is given by eq 1 as the difference between the height of the crossing point ΔE_c

$$\Delta E^{\ddagger} = \Delta E_c - B \quad (1a)$$

$$\Delta E_c = fG \quad (1b)$$

(relative to the reactants' complex R) and the avoided crossing interaction *B*. In addition, by appeal to (1), ΔE_c can be expressed as some fraction, *f*, of the diagram gap, *G*, at the reactant's extreme.[2a,b]

Knowledge of the *f*, *G*, and *B* quantities is important therefore for predicting and rationalizing trends in the barrier. This approach has proved very useful for the discussion of the barrier problem in S_N2, and other electrophile-nucleophile reactions.[2a,b,3] In addition, we have already noted that the stability of X_n^z clusters (n = 3, 4, 6; z = 0, −1; X = monovalent atom or group) correlates with gap size.[4] All of these applications have so far relied on qualitative considerations and it becomes essential to test the ideas by rigorous quantitative means which can generate the diagrams and provide insight into the factors that control the variations of the diagram quantities *f*, *G*, and *B*. As discussed in the preceding paper,[5] the multistructure VB method[6] provides the ideal means toward this goal.

In this paper, the multistructure VB method is used to generate the curve-crossing SCD for two prototypical exchange reactions, **2** and **3**, which represent two mechanistic types of atom exchange

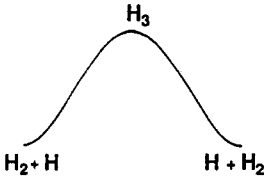

2

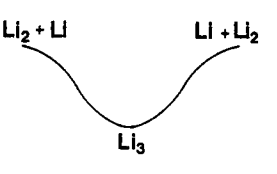

3

reaction, one passing through a potential barrier and the other

(1) Shaik, S. S. *J. Am. Chem. Soc.* **1981**, *103*, 3692.

(2) (a) Shaik, S. S. *Prog. Phys. Org. Chem.* **1985**, *15*, 197. (b) Shaik, S. S. In *New Concepts for Understanding Organic Reactions*; Bertran, J.; Csizmadia, I. G., Eds.; NATO ASI Series; Kluwer: Dordrecht, 1989; Vol. 267, p 165. (c) Pross, A.; Shaik, S. S. *Acc. Chem. Res.* **1983**, *16*, 363. (d) Pross, A. *Adv. Phys. Org. Chem.* **1985**, *21*, 99.

(3) (a) Cohen, D.; Bar, R.; Shaik, S. S. *J. Am. Chem. Soc.* **1986**, *108*, 231. (b) Mitchell, D. J.; Schlegel, H. B.; Shaik, S. S.; Wolfe, S. *Can. J. Chem.* **1985**, *63*, 1642. (c) Buncel, E.; Shaik, S. S.; Um, I. H.; Wolfe, S. *J. Am. Chem. Soc.* **1988**, *110*, 1275. (d) Pross, A. *Acc. Chem. Res.* **1985**, *18*, 212.

(4) (a) Shaik, S. S.; Bar, R. *Nouv. J. Chim.* **1984**, *8*, 411. (b) Shaik, S. S.; Hiberty, P. C.; Ohanessian, G.; Lefour, J.-M. *Nouv. J. Chim.* **1985**, *9*, 385. (c) Shaik, S. S.; Hiberty, P. C.; Lefour, J.-M.; Ohanessian, G. *J. Am. Chem. Soc.* **1987**, *109*, 363. (d) Shaik, S. S.; Hiberty, P. C.; Ohanessian, G.; Lefour, J.-M. *J. Phys. Chem.* **1988**, *92*, 5086.

(5) Maitre, P.; Hiberty, P. C.; Lefour, J.-M.; Ohanessian, G., preceding paper in this issue.

(6) (a) Hiberty, P. C.; Lefour, J.-M. *J. Chim. Phys.* **1987**, *84*, 607. (b) Sevin, A.; Hiberty, P. C.; Lefour, J.-M. *J. Am. Chem. Soc.* **1987**, *109*, 1845.

0022-3654/90/2094-4089$02.50/0

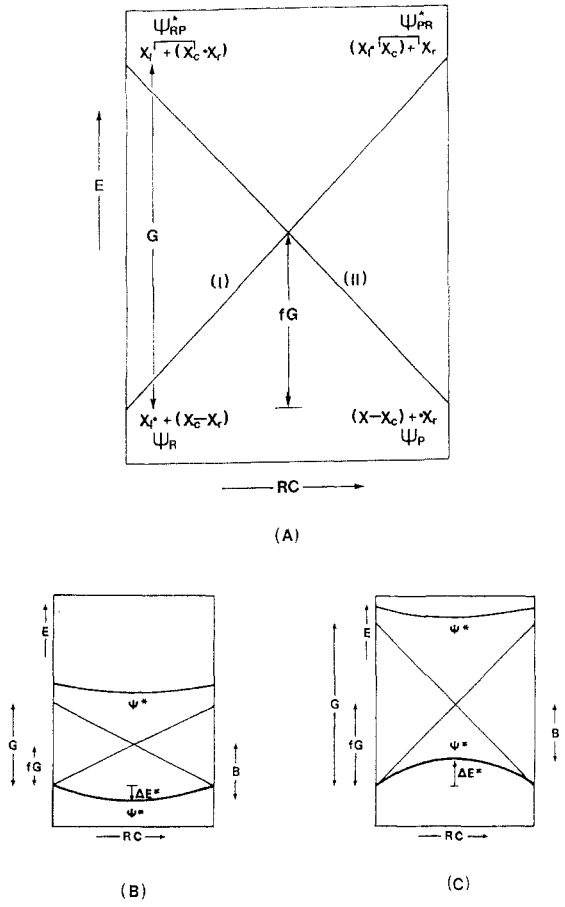

Figure 1. (A) A curve crossing diagram for $X_l^{\bullet} + X_c{-}X_r \rightarrow X_l{-}X_c + X_r^{\bullet}$. G is the diagram gap and fG is the height of the crossing point or the reorganization energy. (B, C) The diagrams with inclusion of avoided crossing. The states after avoided crossing are shown by dark lines. The avoided crossing resonance interaction is B.

involving a stable intermediate. Since avoided crossings have generally been associated with energy *barriers*, the opposite profiles of **2** and **3** pose a fundamental problem and a challenge for the usefulness of the model. Specifically, (i) can the curves in the model be reproduced rigorously and meaningfully? (ii) Can their avoided crossing reproduce the extreme mechanistic behavior in **2** and **3**? (iii) Do the quantitatively determined f, G, and B parameters follow some fundamental property of the atom?

II. The Qualitative Model

The diagram for a three-electron exchange process has been discussed in great detail before[2b,4] and a brief description follows here of the makeup of the curve-crossing diagram.

Consider a general three-electron exchange process as in eq 2, where the subscripts refer to the left-hand side, central, and right-hand side fragments X.

$$X_l^{\bullet} + X_c{-}X_r \rightarrow X_l{-}X_c + X_r^{\bullet} \qquad (2)$$

Figure 1A shows the curve-crossing diagram[4d] without the avoided crossing. Each curve is anchored at a ground state and at an excited VB structure of reactants and products.

The ground states of curves I and II are the usual Lewis structures, where the odd electron is represented by a heavy dot and the bond by a line connecting the bonded atoms. Each Lewis structure is an optimized linear combination of a Heitler–London (H–L) and two zwitterionic structures. These are exemplified in **4**–**6** for the ground state of curve I, with a line connecting the

$$\underset{\textbf{4}\ (\text{H–L})}{X_l^{\bullet}\ \ X_c{-}X_r} \qquad \underset{\textbf{5}}{X_l^{\bullet}\ :X_c^{-}\ X_r^{+}} \qquad \underset{\textbf{6}}{X_l^{\bullet}\ X_c^{+}\ :X_r^{-}}$$

heavy dots in **4** symbolizing the two spin-paired electrons of the H–L configuration.

Each excited structure of the diagram retains the electronic character of the ground state which is at the opposite extreme of the diagram. In this manner each curve describes a uniform spin-pairing situation. Thus, in each excited structure there is an infinitely distant radical, X_l or X_r, singlet-coupled to the X_c atom in the X_2 fragment, while the two electrons in the X_2 fragment are left uncoupled.

For curve I, the wave function of the excited structure reads

$$\Psi^*_{PR} = N[|\varphi_l\bar{\varphi}_c\varphi_r| - |\varphi_l\varphi_c\bar{\varphi}_r|] \qquad (3)$$

where N is a normalization constant. Here the electron spin on X_c is half α and half β (being singlet-coupled to X_r), while the electron spin on X_l is α. The net result is that the X_2 fragment in the excited structure is represented, in terms of the two-electron states of X_2, as a mixture of 25% singlet and 75% triplet. The same holds for curve II, with interchange of the roles of X_l and X_r. This definition of the curves allows them to be variationally calculated at any point of the reaction coordinate. An alternative definition of the excited VB structure is, however, possible, in which X_2 is now a pure triplet. Fuller details of this latter alternative are given in the Appendix.

At intermediate points along the reaction coordinate, curve I is an optimized linear combination of the three configurations **4**–**6** which constitute generally the Lewis wave function. In addition to **4**–**6**, there are two zwitterionic configurations **7** and **8** which can mix into curve I but only at intermediate points along the reaction coordinate. At the two extremes of the reaction coor-

$$\underset{\textbf{7}}{X_l^{+}\ \ X_c^{\bullet}\ :X_r^{-}} \qquad \underset{\textbf{8}}{:X_l^{-}\ \ X_c^{\bullet}\ \ X_r^{+}}$$

dinate the latter two configurations belong to charge-transfer states of the general nature $X^+X_2^{\bullet-}$ and $X{:}^-X_2^{\bullet+}$, which are orthogonal to the anchor points of curves I and II. All the above description applies also to curve II.

The diagram gap is therefore related[4c] to the singlet–triplet excitation of the ground-state molecule in the following way:

$$G \approx 0.75\Delta E_{st}(\text{X–X}) \qquad (4)$$

At finite distances, a mixing occurs between the two wave functions, generating two adiabatic states and an avoided crossing. At the crossing geometry, these two adiabatic states are the corresponding positive and negative combinations of the H–L configurations, and each combination contains in addition a mixture of appropriate symmetry-adapted zwitterionic configurations. The covalent components of these two adiabatic states are the following:

$$\Psi^{\ddagger} = N^{\ddagger}[2|\varphi_l\bar{\varphi}_c\varphi_r| - |\bar{\varphi}_l\varphi_c\varphi_r| - |\varphi_l\varphi_c\bar{\varphi}_r|] \qquad (5)$$

$$\Psi^{*} = N^{*}[|\varphi_l\varphi_c\bar{\varphi}_r| - |\bar{\varphi}_l\varphi_c\varphi_r|] \qquad (6)$$

The pictorial representation of these combinations are **9** and **10** which illustrate that $\Psi^{\ddagger}$ possesses three electrons delocalized

$$\underset{\substack{3e^-\\ \textbf{9}(\Psi^{\ddagger})}}{X_l{-}{-}X_c{-}{-}X_r} \qquad \underset{\textbf{10}(\Psi^{*})}{X_l^{\bullet}\ \ X_c^{\bullet}\ \ {}^{\bullet}X_r}$$

over the three centers, as in allyl radical,[7] while Ψ^* possesses a long bond. Therefore, $\Psi^{\ddagger}$ is the ground state and Ψ^* is the excited state.

The energy difference between $\Psi^{\ddagger}$ and Ψ^* is sensitive to the geometry of the X_3 species. The largest difference occurs at a collinear geometry, while at an equilateral triangular geometry this difference goes to zero.[8]

Let us restrict ourselves to collinear X_3 species and consider the result of the avoided crossing as a function of the nature of the atom X. When X changes all the curve-crossing parameters

(7) (a) Levin, G.; Goddard, W. A., III *J. Am. Chem. Soc.* **1975**, *97*, 1649. (b) Matsen, F. A. *Acc. Chem. Res.* **1978**, *11*, 387. (c) Fox, M. A.; Matsen, F. A. *J. Chem. Educ.* **1985**, *62*, 477.

(8) $\Psi^{\ddagger}$ and Ψ^* are the two degenerate states of the equilateral triangle. See: (a) Albright, T. A.; Burdett, J. K.; Whangbo, M. H. *Orbital Interactions in Chemistry*; Wiley: New York, 1985; p 97. (b) Malrieu, J.-P.; Maynau, D.; Daudey, J.-P. *Phys. Rev.* **1984**, *B30*, 1817.

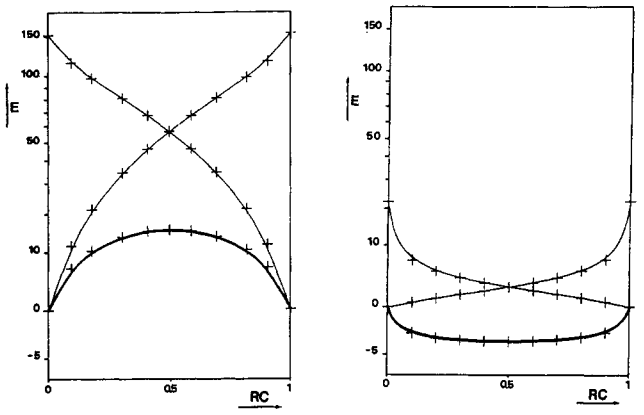

Figure 2. Quantitative curve crossing diagrams. The energy axis is drawn on a logarithmic scale (E in kcal/mol). The heavy line represents the adiabatic curve. (A) The diagram for H_3. (B) The diagram for Li_3.

G, f, and B may change[4d,9] (see **1** and eq 1). It has been postulated, however, that the changes in G dominate all the other changes, as schematized in parts B and C of Figure 1. Thus, when G is large, the ground-state X_3 species is expected to be an unstable species ($\Delta E^{\ddagger} > 0$) as in part B of Figure 1. On the other hand, when the gap is very small, as in part C of Figure 1, the ground-state X_3 species is stable ($\Delta E^{\ddagger} < 0$).

Since the diagram gap is related to the singlet–triplet excitation of the Lewis bond, X–X (eq 4), it is possible to understand the different behaviors of the H and Li exchange reactions, as schematized in **2** and **3**. Thus, ΔE_{st}(H–H) is 250 kcal/mol[10a] while ΔE_{st}(Li–Li) is 32 kcal/mol,[10b,c] and this 8-fold ratio provides a very simple rationale why the H exchange should proceed by passing through H_3 on the top of a barrier, while Li exchange should proceed by passing through an intermediate Li_3 species. The next section discusses the quantitative curve-crossing diagrams and shows the soundness of the above qualitative ideas.

III. Quantitative Curve-Crossing Diagrams for Reactions 1 and 2

Full computational details for the construction of VB structures for X_2 and X_3 (X = H, Li) from VBF's (valence bond functions) are described in sections I, II.E, and II.F of the preceding paper.[5] A brief description of the construction of the curve-crossing diagram is given here. Each of the curves in Figure 1a is generated from a variational calculation over the subset of VBF's that define a single bonding scheme, i.e., a single optimized Lewis structure. Thus, for example, curve I (Figure 1) is computed as a variational linear combination of all the VBF's which contribute to the VB structure **4**–**6** only. These Lewis type linear combinations are recomputed variationally at each point along the reaction coordinate (which is described below in detail) and provide thereby the two variational curves that are displayed in Figure 2, A and B, for X = H and Li.

The diagram gap quantity G is simply the energy difference between the so calculated variational wave functions at the extremes of the reaction coordinate. The corresponding f quantity (Figure 1A) is computed in turn as the ratio of the energy height of the crossing point and G.

The adiabatic X_3 curve is computed as a variational linear combination over the entire set of VBF's that describe the two Lewis structures (**4**–**6** for structure I and symetrically equivalent for II) and the two zwitterionic type structures (**7** and **8**). The diagram quantity B that is reported in Table III is computed as the energy difference between the crossing point and the adiabatic X_3 state. Thus B represents an energy difference between a variational single bonding scheme and adiabatic and delocalized X_3 state.

TABLE I: Reaction Coordinate for the Reaction H + H_2 → H_2 + H[a]

n_1	0.00	0.10	0.18	0.30	0.41	0.50
R_1	∞	1.46	1.26	1.10	1.01	0.95
R_2	0.74	0.77	0.80	0.85	0.90	0.95

[a] Distances are in Å.

TABLE II: Reaction Coordinate for the Reaction Li + Li_2 → Li_2 + Li[a]

n_1	0.00	0.10	0.20	0.30	0.40	0.50
R_1	∞	3.42	3.22	3.11	3.02	2.96
R_2	2.76	2.79	2.82	2.86	2.91	2.96

[a] Distances are in Å.

TABLE III: Diagram Parameters for H_3 and Li_3[a]

	ΔE	G	f	B
H_3	15.3	156.8	0.37	42.4
Li_3	−3.8	22.4	0.13	6.6

[a] ΔE, G, f, and B are in kcal/mol.

A. Reaction Coordinate. Since our purpose is illustrative rather than exhaustive we have chosen to limit the quantitative study to linear H_3 and Li_3. Once this choice is made, the geometry of the crossing point is unique and corresponds to the optimized geometries of the linear species, **11** and **12**. Also unique is the

$$\overset{0.95\text{ Å}}{\text{H---H---H}} \qquad \overset{2.965\text{ Å}}{\text{Li---Li---Li}} \qquad \text{X}_{\text{l}}\text{---X}_{\text{c}}\text{---X}_{\text{r}}$$
$$\qquad\qquad\qquad\qquad\qquad\qquad\qquad\qquad\qquad\qquad\quad n_1 \quad n_2$$
$$\textbf{11} \qquad\qquad\qquad \textbf{12} \qquad\qquad\qquad \textbf{13}$$

energy of this crossing point relative to the reactants, so that the f parameter (eq 1) is independent of the details of the reaction coordinate. Consequently, it has been decided to use a simple procedure to generate a set of intermediate geometries. The reaction coordinate RC is defined from the bond orders n_1 and n_2 in **13** as follows:

$$\text{RC} = \frac{n_1 - n_2 + 1}{2} \tag{7}$$

In this manner the RC varies between zero and unity. In the reactants $n_1 = 1$ and $n_2 = 0$ (see ref 12), so that RC = 0. Using Pauling's definition of the bond orders,[12] we have

$$n_1 = \exp[(R^0_{cr} - R_{cr})/A_{cr}] \tag{8a}$$

$$n_2 = \exp[(R^0_{lc} - R_{lc})/A_{lc}] \tag{8b}$$

where R^0 is the equilibrium bond length of the dimer and R is the actual X–X length. The parameter A_{ij} is a constant characteristic of the X_iX_j bond, and is determined[11] by requiring that at the crossing point ($R = R^{\ddagger}$) the bond orders are 0.5 (which is of course a matter of convenience rather than anything physical). Thus the A_{ij}'s become

$$A_{lc} = A_{cr} = (R^{\ddagger} - R^0)/\ln 2 \tag{9}$$

Among the various possibilities, we have selected the set of geometries which conserve the total bond order, $n_1 + n_2 = 1$ (see ref 11), and which are listed in Tables I and II. This reaction coordinate has been shown by Agmon[13] to be reasonably close to the intrinsic reaction path for atom exchange processes. In any event the chief purpose here is to show that curves I and II of Figure 1 can be computed meaningfully and variationally along a set of distortions between reactant and product geometries.

B. Results. The quantitative curve-crossing diagrams are displayed in Figure 2. Since the orders of magnitude of the $\Delta E^{\ddagger}$,

(9) Malrieu, J.-P. *Nouv. J. Chim.* **1986**, *10*, 61.
(10) (a) Kolos, W.; Wolniewicz, L. *J. Chem. Phys.* **1965**, *43*, 2429. (b) Olson, M. L.; Konowalow, D. D. *Chem. Phys.* **1977**, *21*, 393. (c) Konowalow, D. D.; Olson, M. L. *J. Chem. Phys.* **1979**, *71*, 450.
(11) Johnston, H. S. *Gas Phase Reaction Rate Theory*; Ronald Press: New York, 1966.
(12) Pauling, L. *J. Am. Chem. Soc.* **1947**, *69*, 542.
(13) Agmon, N. *Chem. Phys. Lett.* **1977**, *45*, 343.

G, and B parameters are so different in H_3 and Li_3, we have chosen to plot the diagrams with the energy axis on a logarithmic scale so as to best illustrate the mechanistic modalities, barrier versus energy well.

The essential quantities of each diagram can be read on the corresponding figure. Thus, the diagram gap for H_3 is 156.8 kcal/mol which is 64% of the singlet–triplet excitation for H_2 (245 kcal/mol with our basis set). On the other hand, the gap for Li_3 is 22.4 kcal/mol and is 68% of the singlet–triplet excitation of Li_2 (32.9 kcal/mol). It is seen that in both cases the gaps are related to the singlet–triplet excitation of the dimer by a factor which is close to the one predicted by the qualitative picture (see the factor 0.75 in eq 4). The deviations are due to the neglect of AO overlap in the qualitative considerations, and if overlap is retained these deviations can be accounted for.[4c,14]

What is probably of major interest here is the correlation between the energy of the trimer relative to reactants or products and the diagram gap. Thus, as predicted qualitatively in parts B and C of Figure 1, the result of the avoided crossing in the case of a large gap is a barrier, while that of a small gap is an intermediate. Since the size of the gap depends on one fundamental property of the atom, its binding strength, it becomes possible to conceptualize a large body of similar data in terms of a single fundamental property of the atom.[4d] In particular, the model also applies to halogen and coinage metal trimers, in which the constituent atoms can be considered as bringing one electron each.

The other diagram parameters, B and f, are found to vary significantly between H_3 and Li_3. Thus for H_3 with the large gap we obtain a large B value, while for Li_3 with the small gap we obtain a small B. Similarly, the f values vary in relation to the gap, being 0.37 for H_3 and 0.13 for Li_3. This variation of all parameters may render the qualitative model difficult to apply, though quantitatively the H_3–Li_3 dichotomy is reproduced by the model. It is essential to understand why despite this variation in the three parameters it is G that appears to be the dominant factor in H_3, Li_3, and other X_3 species.[4c,d] We therefore return to the qualitative model to understand the dependence of B and f on the nature of X.

IV. Back to the Qualitative Model

In much the same way as eq 5 for G, simple expressions for B can be obtained by use of the effective Heisenberg Hamiltonian VB theory,[9,15] the DIM method,[14,16] or the recently discussed one-electron-approximation VB method.[2b] The simplest method to use is the former, which leads to the following expression[9] for B (neglecting again AO overlap)

$$B = (1/4)\Delta E_{st}'(\text{X–X}) \tag{10}$$

where $\Delta E_{st}'(\text{X–X})$ is the singlet–triplet energy gap of the X–X dimer with an X–X distance equal to $R^{\ddagger}$. Similar expressions are obtained by the DIM method[4d,14] and by the one-electron-approximation method.[2b] In each case B is related to the singlet–triplet splitting of a dimer X–X at the distance that corresponds to the crossing point. The $\Delta E_{st}'(\text{X–X})$ values are 177 kcal/mol for H and 23 kcal/mol for Li, respectively. These values are seen to parallel the singlet–triplet excitation of the corresponding dimers at their equilibrium geometries, and this is the cause for the relation between the diagram gap G and the avoided crossing interaction B. Indeed if eq 10 is used with the computed $\Delta E_{st}'$ values, the resulting B values are 44 and 6 kcal/mol for the H_3 and Li_3 species, respectively, reasonably close to the quantitatively computed values. What clearly emerges then is that the avoided crossing interaction is related to the singlet–triplet gap in the X–X dimer, which in most cases correlates with the binding strength of the atom X.

Let us turn to the quantity f which is related to G and to the height of the crossing point by eq 1b. Using again the effective Hamiltonian method[9] it is possible to derive an expression for f by appeal to the parameters ΔE_{st} and E_T of the dimer X–X, as illustrated in **14**. Here, ΔE_{st} is the singlet–triplet splitting while

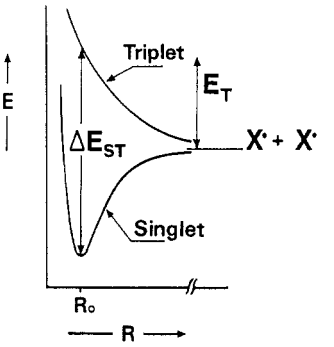

14

E_T is the triplet repulsion. Using these parameters and eq 11 we obtain

$$f = \frac{4(2E_T' - E_T) - 5\Delta E_{st}'}{3\Delta E_{st}} + \frac{4}{3} \tag{11}$$

Here the primed quantities refer to the corresponding values at the geometry of the dimer fragment at the crossing point, and the unprimed ones refer to the corresponding values at the equilibrium dimer bond length.

E_T or E_T' can be expressed as fractions, α, of the corresponding singlet–triplet gaps, ΔE_{st} and $\Delta E_{st}'$, that is,

$$E_T = \alpha \Delta E_{st} \tag{12}$$

For strong binders like H, α is close to 0.5 or slightly larger,[9] while for weak binders like Li α is much smaller than 0.5. Using eqs 11 and 12 an expression for f becomes

$$f = \frac{(8\alpha - 5)\Delta E_{st}'}{3\Delta E_{st}} - \frac{4}{3}(\alpha - 1) \tag{13}$$

The derivative of f with respect to α, in eq 14, shows that f

$$\frac{df}{d\alpha} = \frac{8\Delta E_{st}'}{3\Delta E_{st}} - \frac{4}{3} \tag{14}$$

decreases as α decreases provided that the ratio $\Delta E_{st}'/\Delta E_{st}$ is larger than 0.5, a condition which is expected to be met for any type of realistic transition state or stable intermediate. In fact, in this study these ratios are 22/33 and 174/245 respectively for Li and H.

Equation 13 can be further used to obtain orders of magnitude for the expected f values. Starting with hydrogens, we take α = 0.5 which leads to f = 0.33 at the limit of very tight geometry, for which $\Delta E_{st}' = \Delta E_{st}$, and a value of 0.5 for an unrealistically loose geometry corresponding to $\Delta E_{st}' = 0.5\Delta E_{st}$. Since the H_3 transition state is between these tight and loose limits, we expect for strong binders $0.33 < f < 0.5$. Using the same procedure for Li leads to smaller f values because α is smaller than 0.5. Thus, it is the ratio between the triplet repulsion and singlet binding energy of a dimer X–X that eventually determines the magnitude of f in the diagram.

This behavior of f can be couched in terms of the mechanism of crossing in Figure 1. Thus, since for Li the repulsive interaction is small (as expressed by $\alpha < 0.5$ (eq 12)) then Li can approach Li_2 very closely along curve I (Figure 1) without significantly raising the energy. For the same approach, the excited pseudostate of curve II descends more steeply owing to the bond making interaction which is stronger than the triplet repulsion. The net result is that the two curves achieve crossing at quite a low energy and tight geometry, and this corresponds to a small f value (eq 1b). For the case of H, the situation is the exact opposite, since the repulsive interaction is large (as expressed by $\alpha > 0.5$ in eq 12). The net result is that the crossing point for H_3 is obtained at proportionally higher energy and looser geometry[17] than the

(14) Maitre, P. DEA Thesis, Université de Paris-Sud, Orsay, France, 1987.
(15) Durand, P.; Malrieu, J.-P. *Adv. Chem. Phys.* **1987**, *67*, 321.
(16) (a) Ellison, F. O.; Huff, N. T.; Patel, J. C. *J. Am. Chem. Soc.* **1963**, *85*, 3544. (b) Companion, A. L. *J. Chem. Phys.* **1968**, *48*, 1186.

corresponding point in Li_3, and hence $f(H_3) > f(Li_3)$.

The variation of f appears to be a crucial factor for the mechanistic modality of H_3 and Li_3. Had it been the case that f was a constant then $\Delta E^{\ddagger}$ in eq 1 would have simply been proportional to G, with all the reactions having a unimodal mechanism, e.g., a barrier which gradually decreases with G. It is the variation of f that causes the reorganization energy term, fG (eq 1) to have a double dependency on ΔE_{st}. This, in turn leads to two main results. First, fG decreases faster than B in eq 1, so that, in a series of X_3 species with a gradually decreasing G, a point is reached where B exceeds the reorganization term fG and an intermediate is formed. Second, the changes in f and B compensate each other in eq 1 and *the net result is that G remains the dominant factor of the X_3 stability and of the mechanistic modality*. This makes the qualitative model an ideal tool for making predictions regarding a large body of data, as has been demonstrated previously.[4]

It must be emphasized though that in other problems, e.g., four-electron problems like S_N2 reactions, the variations of f and B appear not to be as found here for the three-electron problem.[2] Yet in each case, as we have shown here the f and B properties follow from considerations of bonding and repulsive interactions.

V. Conclusion

The present study indicates that curve crossing diagrams[1-4] can be computed with a satisfactory degree of accuracy which is comparable to Hartree–Fock computations with an extended basis set, followed by a decent CI treatment.

The curve-crossing diagram model provides very useful insight into the mechanism of atom exchange reactions (**2** vs **3**). The diagram's quantities are G, f, and B, where fG constitutes the reorganization energy required to achieve crossing and B is the avoided crossing resonance interaction. The qualitative analysis shows, and the quantitative computations affirm, that *these diagram properties are all related to a single fundamental property of X, the singlet–triplet splitting, ΔE_{st}, of the dimer*. It is possible therefore to rationalize and predict a large body of X_3 data by simply relying on a single fundamental property of the reactants, $\Delta E_{st}(X–X)$.[4c,d] Thus, when ΔE_{st} is large, the X_3 species is an unstable transition state with loose bonds[17] and a large B property. On the other hand, when ΔE_{st} is small, X_3 is a stable intermediate with tight bonds[17] and a small B property.

The avoided crossing interaction B is an important quantity on two counts. First, the computations show that B is small in relation to G, so that the final adiabatic curve stays reasonably close to the diabatic curves; this allows reasoning reactivity on the basis of the features of the diabatic curves. Second, B constitutes the quantum mechanical resonance energy (QMRE)[4c,d] of the X_3 species. Since resonance energies are important quantities in chemical reasonings, it is essential to devise methods which compute QMRE reliably and meaningfully. The present work computes the QMRE as the energy difference between a variational bonding scheme and the variational adiabatic and delocalized ground state. As such, the methodology provides a unique value for the QMRE (B). Finally, the analysis projects that the QMRE is a property of both stable as well as unstable X_3 species.

Appendix

The definition that we have used for the excited VB structures, in the computations presented in this work, emphasizes the use of a single bonding scheme for each crossing curve. Another definition has been proposed recently, in which the excited VB structures at the upper anchor points of the diagram are composed of a dimer X–X in a pure triplet state and an infinitely distant X_r radical.[4a] The wave function $\Psi_{PR}{}^*$ for such a structure is (A1).

$$\Psi_{PR}{}^* = N^*[2|\varphi_l\varphi_c\bar{\varphi}_r| - |\bar{\varphi}_l\varphi_c\varphi_r| - |\varphi_l\bar{\varphi}_c\varphi_r|] \qquad (A1)$$

Here X_r is singlet-coupled to X_l and X_c 50% each. This excited state can be connected to the ground-state Ψ_P of the products by a nonadiabatic curve. However, such curves cannot be calculated variationally but must be generated by rotations among the space of the adiabatic states $\Psi^{\ddagger}$ and Ψ^*. Such a procedure has recently been used by Malrieu and collaborators[18] for H_3^-.

Since the excited structure contains a dimer in a pure triplet state, the diagram gap G is now equal to the vertical singlet–triplet excitation energy of the dimer (A2). An interesting feature of

$$G = \Delta E_{st}(X–X) \qquad (A2)$$

this definition is that nonadiabatic states match the adiabatic ones at reactant and product geometries. This makes the diagram easier to use qualitatively.

Thus there are two possible definitions of the nonadiabatic curves, one being better suited for quantitative calculations (eq 3) and the other simpler to use in qualitative reasonings. It should be emphasized however that in both versions the gap G is proportional to the singlet–triplet energy gap ΔE_{st} of X_2 (with a factor of either 3/4 or 1). The singlet–triplet gap of X_2, being either G or $(3G/4)$, emerges in both cases as the key property against which the trimer energies can be ordered and explained.

Registry No. H, 12385-13-6; H_2, 1333-74-0; Li, 7439-93-2; Li_2, 14452-59-6.

(17) The term looser refers to the percentage of bond stretching in X_3 vs X_2. For X = H this percentage is 29%, while for X = Li, it is 7%.

(18) Kabbaj, O. K.; Volatron, F.; Malrieu, J.-P. *Chem. Phys. Lett.* **1988**, *147*, 353.